# High-speed Nonsingular Terminal Switched Sliding Mode Control of Robot Manipulators

Fengning Zhang

***Abstract*—This paper proposes a high-speed nonsingular terminal switched sliding mode control (HNT-SSMC) strategy for robot manipulators. The proposed approach enhances the control system performance by switching among appropriate sliding mode controllers according to different control demands in different regions of the state space. It is shown that the high-speed nonsingular terminal switched sliding mode (HNT-SSM) which is the representation of different control demands and enforced by the HNT-SSMC has the property of global high-speed convergence compared with the nonsingular fast terminal sliding mode (NFTSM), and provides the global non-singularity. The simulation study of an application example is carried out to validate the effectiveness of the proposed strategy.**

***Index Terms*—Finite-time stability, nonlinear systems, robot control, sliding mode control (SMC), switched control.**

## I. Introduction

MANY control strategies which are capable of being applied in the control of robot manipulators can be found in the literature; which include adaptive control [1], [2], optimal control [3], backstepping [4], sliding mode control [5], and switched control [6]. Switched control, which has attracted extensive attention in both theoretical studies and applications [7]−[9], is one of the effective approaches to enhancing performance [10], [11]. In practice it is very common to meet different control demands in different regions of the state space. For this reason, a novel high-speed nonsingular terminal switched sliding mode control (HNT-SSMC) strategy, which allows enhancing the control performance by switching among appropriate sliding mode controllers according to each region of the state space, is proposed in this paper for the control of robot manipulators.

Sliding mode control (SMC) also has attracted a great amount of interest due to its advantages, such as strong robustness, rapid response, better transient performance, order reduction, and easiness to design and implement [12], [13]. In literatures, various SMC applications can be seen, for example, uncertain nonlinear systems [14]−[16], induction motors [17], hypersonic vehicles [18]−[20], and observers [21]−[23]. SMC is designed to drive and constrain the system state to the sliding mode surface that is defined based on the convergence requirements, in which the closed-loop response becomes totally insensitive to any uncertainty. A characteristic of conventional SMC is that the system state converges to the equilibrium point in infinite time due to the linear sliding mode manifold that is asymptotically stable.

Terminal sliding mode control is one of the effective finite-time control methods which are frequently employed. Terminal sliding mode (TSM) control [24] has been developed to offer some superior properties compared with the conventional linear sliding-mode control, such as fast and finite-time convergence and higher control precision. However, TSM control has singularity and has slow convergence speed when the system state is at a distance from the equilibrium. Aiming at avoiding the singularity problem in TSM control systems, a non-singular terminal sliding mode (NTSM) control [5] was proposed. To solve the problem of slow convergence speed when the system state is at a distance from the equilibrium in TSM, there appeared fast terminal sliding mode (FTSM) control [25]. Recently, a nonsingular fast terminal sliding mode (NFTSM) control [26], which does not have both the problems of TSM control, was proposed to offer the singularity avoidance and fast convergence speed when being at a distance from the equilibrium.

In this paper, it is shown that the high-speed nonsingular terminal switched sliding mode (HNT-SSM) which is the representation of different control demands in the different regions of the state space and also enforced by the HNT-SSMC, possesses the property of global high-speed convergence compared with the NFTSM, and provides the global non-singularity. The simulation investigation of an application example is conducted to verify the theoretical analysis and the effectiveness of the proposed approach.

The rest of this paper is organized as follows. The proposed approach for robot manipulators is introduced in Section II. The stability and convergence analysis are presented in Section III. In Section IV the performance analysis is given. The simulation study is conducted in Section V, and Section VI concludes this paper.

## II. High-speed Nonsingular Terminal Switched Sliding Mode Control

In this section, a high-speed nonsingular terminal switched sliding mode control is developed for the $n$-link robot manipulator

$$M(q)\ddot{q} + C(q,\dot{q}) + G(q) = \tau + \tau_d \tag{1}$$

Manuscript received May 20, 2015; accepted November 13, 2015. This work was supported partially by the Research Program of Science and Technology at Universities of Inner Mongolia Autonomous Region (NJZY13279). Recommended by Associate Editor Qinglai Wei.

Citation: F. N. Zhang, "High-speed nonsingular terminal switched sliding mode control of robot manipulators," *IEEE/CAA J. of Autom. Sinica*, vol. 4, no. 4, pp. 775−781, Oct. 2017.

F. N. Zhang is with the Department of Physics, Jining Normal University, Wulanchabu 012000, China (e-mail: zfn010@gmail.com).

Color versions of one or more of the figures in this paper are available online at http://ieeexplore.ieee.org.

Digital Object Identifier 10.1109/JAS.2016.7510157

where $q = (q_1, \ldots, q_m)^T \in \mathbb{R}^m$ is the vector of joint angular position, $M(q) = M_0(q) + \delta M(q) \in \mathbb{R}^{m\times m}$ is the positive definite inertia matrix, $C(q,\dot{q}) = C_0(q,\dot{q}) + \delta C(q,\dot{q}) \in \mathbb{R}^m$ is the vector of centripetal and coriolis forces, $G(q) = G_0(q) + \delta G(q) \in \mathbb{R}^m$ is the vector of gravitational torques, $\tau \in \mathbb{R}^m$ is the vector of applied joint torque and $\tau_d \in \mathbb{R}^m$ is the vector of bounded external disturbance with $\|\tau_d\| \le \bar{\tau}_d$. Here $M_0(q)$, $C_0(q,\dot{q})$, and $G_0(q)$ are the nominal parts, whereas $\delta M(q)$, $\delta C(q,\dot{q})$, and $\delta G(q)$ are uncertain parts. $F(q,\dot{q},\ddot{q}) = -\delta M(q)\ddot{q} - \delta C(q,\dot{q}) - \delta G(q) \in \mathbb{R}^m$ is the lumped system uncertainty, and the assumption in [5] is adopted here, $\|F(q,\dot{q},\ddot{q})\| \le b_0 + b_1\|q\| + b_2\|\dot{q}\|^2 = \bar{F}$.

Let $q_r = (q_{1r}, \ldots, q_{mr})^T \in \mathbb{R}^m$ be a twice differentiable trajectory, and define $e_1 = q_r - q = (e_1^{(1)}, e_2^{(1)}, \ldots, e_m^{(1)})^T \in \mathbb{R}^m$, $e_2 = \dot{q}_r - \dot{q} = (e_1^{(2)}, e_2^{(2)}, \ldots, e_m^{(2)})^T \in \mathbb{R}^m$, then the error equation of the robot manipulator can be obtained as follows:

$$\begin{aligned}\dot{e}_1 &= e_2\\ \dot{e}_2 &= \ddot{q}_r + M_0^{-1}(q)\left(C_0(q,\dot{q}) + G_0(q)\right) - M_0^{-1}(q)\,\tau\\ &\quad - M_0^{-1}(q)\left(F + \tau_d\right)\end{aligned} \tag{2}$$

in which $d(e_1,e_2,t) = -M_0^{-1}(q)(F+\tau_d)$, $\|d(e_1,e_2,t)\| \le \bar{d}(e_1,e_2,t) = \|M_0^{-1}(q)\|(\bar{F}+\bar{\tau}_d)$.

The phase planes $E_k$ $(k = 1,2,\ldots,m)$ of system (2) are partitioned into regions $\Omega_{\hat{i}}^k$ $(\hat{i} = 0,1,2,3)$, where

$$\begin{aligned}E_k &:= \left\{(e_k^{(1)}, \dot{e}_k^{(1)}) : (e_k^{(1)}, \dot{e}_k^{(1)}) \in \mathbb{R}^2\right\}\\ \Omega_1^k &:= \left\{(e_k^{(1)}, \dot{e}_k^{(1)}) \in E_k : |e_k^{(1)}| \in [c_1^{(k)}, c_2^{(k)})\right\}\\ \Omega_2^k &:= \left\{(e_k^{(1)}, \dot{e}_k^{(1)}) \in E_k : |e_k^{(1)}| \in [c_1^{(k)}, c_3^{(k)})\right\}\\ \Omega_3^k &:= \left\{(e_k^{(1)}, \dot{e}_k^{(1)}) \in E_k\right\},\quad \Omega_0^k := \emptyset\end{aligned}$$

with $c_1^{(k)} = 0$, $c_2^{(k)} = \delta_k \in (0,1)$, $c_3^{(k)} = 1$, and $c_4^{(k)} > 1$. Further, the regions $E_i^k$ are introduced via $E_i^k := \Omega_i^k \backslash \Omega_{i-1}^k$, where $i = 1,2,3$, $k = 1,2,\ldots,m$ (see Fig. 1).

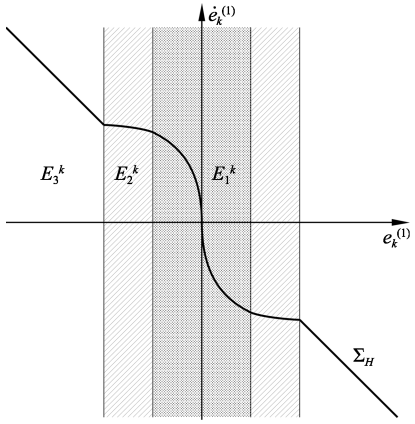


Fig. 1. Examples of the phase plane partitioning and the HNT-SS manifold.

The HNT-SSMC designed for the robot manipulator is

$$\tau_H :\quad \tau_{\sigma(E(t))} \tag{3}$$

where

$$\tau_{\sigma(E(t))} := M_0(q)(\ddot{q}_r + M_0^{-1}(q)(C_0(q,\dot{q}) + G_0(q)) + v_{\sigma(E(t))})$$

$\nu_{\sigma(E(t))} := (\nu_{\sigma_1(E_1(t))}^{(1)}, \nu_{\sigma_2(E_2(t))}^{(2)}, \ldots, v_{\sigma_m(E_m(t))}^{(m)})^T$ is the switching part of the HNT-SSMC, $E_k(t) := (e_k^{(1)}(t), \dot{e}_k^{(1)}(t))$ denotes the projection of the system state onto the plane $E_k$,

$$\sigma_k(E_k(t)) : [0,+\infty) \to I := \{1,2,3\}$$

serves as the switching signal,

$$\begin{aligned}v_{i^*}^{(k)} := {}& \beta_k^{\frac{1}{\gamma_{i^*}^{(k)}}}(\alpha_{i^*}^{(k)})^{\frac{1}{\gamma_{i^*}^{(k)}}}\gamma_{i^*}^{(k)}|\dot{e}_k^{(1)}|^{2-\frac{1}{\gamma_{i^*}^{(k)}}}\mathrm{sgn}(\dot{e}_k^{(1)})\\ &+ h_{i^*}^{(k)}s_{i^*}^{(k)} + \eta_{i^*}^{(k)}\mathrm{sgn}(s_{i^*}^{(k)}) + \bar{d}\mathrm{sgn}(s_{i^*}^{(k)})\end{aligned}$$

and

$$v_{i*}^{(k)} := \beta_k\dot{e}_k^{(1)} + h_{i*}^{(k)}s_{i*}^{(k)} + \eta_{i*}^{(k)}\mathrm{sgn}(s_{i*}^{(k)}) + \bar{d}\mathrm{sgn}(s_{i*}^{(k)})$$

are the components of the switching part $\nu_{\sigma(E(t))}$,

$$s_{i^*}^{(k)} := e_k^{(1)} + \frac{1}{\beta_k^{\frac{1}{\gamma_{i^*}^{(k)}}}(\alpha_{i^*}^{(k)})^{\frac{1}{\gamma_{i^*}^{(k)}}}}|\dot{e}_k^{(1)}|^{\frac{1}{\gamma_{i^*}^{(k)}}}\mathrm{sgn}(\dot{e}_k^{(1)})$$

and

$$s_{i*}^{(k)} := \dot{e}_k^{(1)} + \beta_k e_k^{(1)}$$

are the components of the HNT-SS variable which will be defined later, $\gamma_1^{(k)} \in (0.5,1)$, $\alpha_1^{(k)} = \delta_k^{\gamma_2^{(k)}-\gamma_1^{(k)}}$, $\gamma_2^{(k)} \in [0,0.5]$, $\alpha_2^{(k)} = 1$, $i^* = 1,2$, $i_* = 3$, $\beta_k$, $\eta_i^{(k)}$, and $h_i^{(k)}$ belong to $\mathbb{R}^+$, $i = 1,2,3$, $k = 1,2,\ldots,m$.

The HNT-SS variable is defined as

$$s_H :\quad s_{\sigma(E(t))} \tag{4}$$

where $s_{\sigma(E(t))} := (s_{\sigma_1(E_1(t))}^{(1)}, s_{\sigma_2(E_2(t))}^{(2)}, \ldots, s_{\sigma_m(E_m(t))}^{(m)})^T$ and $s_H := (s_H^{(1)}, s_H^{(2)}, \ldots, s_H^{(m)})^T$.

The HNT-SSM is defined as

$$S_H :\quad s_{\sigma((E(t))} = 0. \tag{5}$$

The corresponding HNT-SS manifold is

$$\Sigma_H : \{(e_1^T, e_2^T) \in \mathbb{R}^{2m} : s_{\sigma(E(t))} = 0\} \tag{6}$$

where $k = 1,2,\ldots,m$.

The scheduling strategy of the HNT-SSMC and the HNT-SSM is

$$\text{if}\ \ E_k(t) \in E_i^k\ \ \text{then}\ \ \sigma_k(E_k(t)) = i$$

where $i = 1,2,3$, $k = 1,2,\ldots,m$.

*Remark 1:* Each of the phase planes is partitioned into three sub-regions, and in every sub-region, there is a sub-manifold (see Fig. 1). The integrated HNT-SS manifold, which is continuous and piecewise smooth, possesses the property of global high-speed convergence and provides the global non-singularity, which is illustrated in Section IV.

*Remark 2:* The chattering phenomenon is caused by the sgn functions in (3). In order to eliminate chattering, the boundary layer method [13] can be used in the controller.

## III. Stability and Convergence Analysis

This section will present the stability and the convergence of the HNT-SSMC. The partitioning of the phase planes of system (2) is introduced as follows (see Fig. 2).

$$ {}^{k}E_j^i := \left\{ \left( e_k^{(1)}, \dot{e}_k^{(1)} \right) \in E_i^k : (-1)^{j+1} e_k^{(1)} \geq 0 \right\} \tag{7} $$

$$ {}^{k}\Sigma_j^i := \left\{ \left( e_k^{(1)}, \dot{e}_k^{(1)} \right) \in {}^{k}E_j^i : s_i^{(k)} = 0 \right\} \tag{8} $$

$$ {}^{k}E_{1j}^i := \left\{ \left( e_k^{(1)}, \dot{e}_k^{(1)} \right) \in {}^{k}E_j^i : (-1)^{j+1} \dot{e}_k^{(1)} \geq 0 \right\} \tag{9} $$

$$ {}^{k}\Lambda_j^i := \left\{ \left( e_k^{(1)}, \dot{e}_k^{(1)} \right) \in E_k : e_k^{(1)} = (-1)^{j+1} c_{i+1}^{(k)} \right\} \tag{10} $$

$$ {}^{k}\bar{E}_j^i := {}^{k}E_j^i \bigcup {}^{k}\Lambda_j^i \tag{11} $$

$$ {}^{k}E_{2j}^i := \left\{ \begin{array}{l} \left( e_k^{(1)}, \dot{e}_k^{(1)} \right) \in {}^{k}\bar{E}_j^i : (-1)^{j+1} \dot{e}_k^{(1)} \leq 0, \\ e_k^{(1)} \neq (-1)^{j+1} c_i^{(k)}, (-1)^{j+1} s_i^{(k)} > 0 \end{array} \right\} \tag{12} $$

$$ {}^{k}E_{3j}^i := \left\{ \left( e_k^{(1)}, \dot{e}_k^{(1)} \right) \in {}^{k}\bar{E}_j^i : e_k^{(1)} \neq (-1)^{j+1} c_i^{(k)}, \; (-1)^{j+1} s_i^{(k)} < 0 \right\} \tag{13} $$

$$ {}^{k}\hat{E}_{2j}^i := \left\{ \left( e_k^{(1)}, \dot{e}_k^{(1)} \right) \in {}^{k}E_{2j}^i : \dot{e}_k^{(1)} = 0 \right\} \tag{14} $$

$$ {}^{k}\tilde{E}_{2j}^i := {}^{k}E_{2j}^i \setminus {}^{k}\hat{E}_{2j}^i \tag{15} $$

where $i = 1, 2, 3$, $j = 1, 2$, and $k = 1, 2, \ldots, m$.

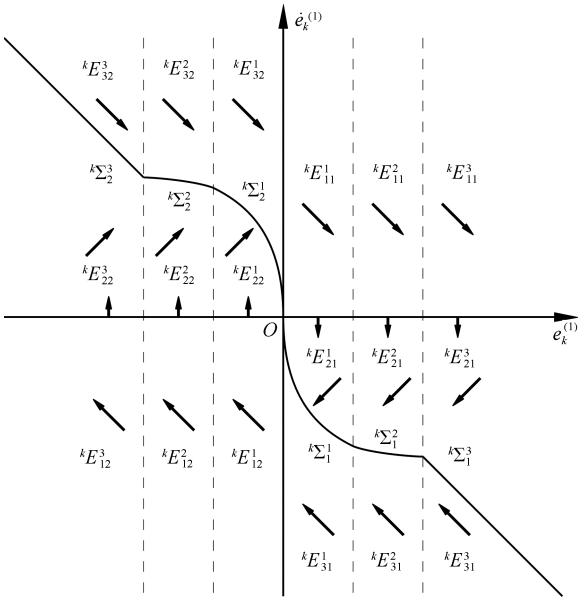


Fig. 2. Examples of the partitioning of the phase planes and the vector fields $\dot{E}_k(t)$.

There are

$$ \begin{aligned} \ddot{e}_k^{(1)} = & -\beta_k^{\frac{1}{\gamma_{i^*}^{(k)}}} (\alpha_{i^*}^{(k)})^{\frac{1}{\gamma_{i^*}^{(k)}}} \gamma_{i^*}^{(k)} |\dot{e}_k^{(1)}|^{2-\frac{1}{\gamma_{i^*}^{(k)}}} \operatorname{sgn}(\dot{e}_k^{(1)}) \\ & - h_{i^*}^{(k)} s_{i^*}^{(k)} - \eta_{i^*}^{(k)} \operatorname{sgn}(s_{i^*}^{(k)}) - \bar{d} \operatorname{sgn}(s_{i^*}^{(k)}) + [d]_k \end{aligned} \tag{16} $$

$$ \begin{aligned} \ddot{e}_k^{(1)} = & -\beta_k \dot{e}_k^{(1)} - h_{i_*}^{(k)} s_{i_*}^{(k)} - \eta_{i_*}^{(k)} \operatorname{sgn}(s_{i_*}^{(k)}) \\ & - \bar{d} \operatorname{sgn}(s_{i_*}^{(k)}) + [d]_k. \end{aligned} \tag{17} $$

For $E_k(t) \in E_i^k$, consider the Lyapunov functions

$$ V_i^{(k)} = \frac{1}{2} s_i^{(k)^2} \tag{18} $$

where $i = 1, 2, 3$, and $k = 1, 2, \ldots, m$. According to (16) and (18), there are

$$ \begin{aligned} \dot{V}_{i^*}^{(k)} &= s_{i^*}^{(k)} \dot{s}_{i^*}^{(k)} \\ &= s_{i^*}^{(k)} \left( \dot{e}_k^{(1)} + \frac{1}{\beta_k^{\frac{1}{\gamma_{i^*}^{(k)}}} \alpha_{i^*}^{(k)^{\frac{1}{\gamma_{i^*}^{(k)}}}} \gamma_{i^*}^{(k)}} |\dot{e}_k^{(1)}|^{\frac{1}{\gamma_{i^*}^{(k)}} - 1} \ddot{e}_k^{(1)} \right) \\ &= -\frac{1}{\beta_k^{\frac{1}{\gamma_{i^*}^{(k)}}} (\alpha_{i^*}^{(k)})^{\frac{1}{\gamma_{i^*}^{(k)}}} \gamma_{i^*}^{(k)}} |\dot{e}_k^{(1)}|^{\frac{1}{\gamma_{i^*}^{(k)}} - 1} \\ &\quad \times \left( h_{i^*}^{(k)} (s_{i^*}^{(k)})^2 + \eta_{i^*}^{(k)} |s_{i^*}^{(k)}| + \bar{d} |s_{i^*}^{(k)}| - [d]_k s_{i^*}^{(k)} \right) \\ &\leq -\frac{1}{\beta_k^{\frac{1}{\gamma_{i^*}^{(k)}}} (\alpha_{i^*}^{(k)})^{\frac{1}{\gamma_{i^*}^{(k)}}} \gamma_{i^*}^{(k)}} |\dot{e}_k^{(1)}|^{\frac{1}{\gamma_{i^*}^{(k)}} - 1} \\ &\quad \times \left( h_{i^*}^{(k)} s_{i^*}^{(k)^2} + \eta_{i^*}^{(k)} |s_{i^*}^{(k)}| \right) \leq 0 \end{aligned} \tag{19} $$

where $k = 1, 2, \ldots, m$. According to (17) and (18), there are

$$ \begin{aligned} \dot{V}_{i_*}^{(k)} &= s_{i_*}^{(k)} \dot{s}_{i_*}^{(k)} \\ &= s_{i_*}^{(k)} (\ddot{e}_k^{(1)} + \beta_k \dot{e}_k^{(1)}) \\ &= -h_{i_*}^{(k)} (s_{i_*}^{(k)})^2 - \eta_{i_*}^{(k)} |s_{i_*}^{(k)}| - \bar{d} |s_{i_*}^{(k)}| + [d]_k s_{i_*}^{(k)} \\ &\leq -h_{i_*}^{(k)} (s_{i_*}^{(k)})^2 - \eta_{i_*}^{(k)} |s_{i_*}^{(k)}| \leq 0 \end{aligned} \tag{20} $$

where $k = 1, 2, \ldots, m$.

The planes $\dot{E}_k$ corresponding to $E_k$ and the regions of $\dot{E}_k$ $(k = 1, 2, \ldots, m)$ are defined as follows

$$ \dot{E}_k := \left\{ (\dot{e}_k^{(1)}, \ddot{e}_k^{(1)}) : (\dot{e}_k^{(1)}, \ddot{e}_k^{(1)}) \in \mathbb{R}^2 \right\} \tag{21} $$

$$ \dot{E}_{\mathrm{II}}^k := \left\{ (\dot{e}_k^{(1)}, \ddot{e}_k^{(1)}) \in \dot{E}_k : \dot{e}_k^{(1)} > 0, \ddot{e}_k^{(1)} < 0 \right\} \tag{22} $$

$$ \dot{E}_{\mathrm{IV}}^k := \left\{ (\dot{e}_k^{(1)}, \ddot{e}_k^{(1)}) \in \dot{E}_k : \dot{e}_k^{(1)} < 0, \ddot{e}_k^{(1)} > 0 \right\} \tag{23} $$

$$ \dot{E}_{\mathrm{VA}^-}^k := \left\{ (\dot{e}_k^{(1)}, \ddot{e}_k^{(1)}) \in \dot{E}_k : \dot{e}_k^{(1)} = 0, \ddot{e}_k^{(1)} < 0 \right\} \tag{24} $$

$$ \dot{E}_{\mathrm{VA}^+}^k := \left\{ (\dot{e}_k^{(1)}, \ddot{e}_k^{(1)}) \in \dot{E}_k : \dot{e}_k^{(1)} = 0, \ddot{e}_k^{(1)} > 0 \right\} \tag{25} $$

$$ \dot{E}_{\mathrm{HD}^-}^k := \left\{ (\dot{e}_k^{(1)}, \ddot{e}_k^{(1)}) \in \dot{E}_k : \dot{e}_k^{(1)} < 0 \right\} \tag{26} $$

$$ \dot{E}_{\mathrm{HD}^+}^k := \left\{ (\dot{e}_k^{(1)}, \ddot{e}_k^{(1)}) \in \dot{E}_k : \dot{e}_k^{(1)} > 0 \right\}. \tag{27} $$

The vector fields $\dot{E}_k(t)$, the derivatives of $E_k(t)$ are defined as

$$ \dot{E}_k(t) := \left( \dot{e}_k^{(1)}(t), \ddot{e}_k^{(1)}(t) \right) \tag{28} $$

where $k = 1, 2, \ldots, m$. Thus, according to (16) and (17), we can have the following conclusions (see Fig. 2), where $k = 1, 2, \ldots, m$:

1) $\dot{E}_k(t) \in \dot{E}_{\mathrm{II}}^k$, if $E_k(t) \in \bigcup_{i \in I} ({}^{k}E_{11}^i \bigcup {}^{k}E_{32}^i)$;
2) $\dot{E}_k(t) \in \dot{E}_{\mathrm{IV}}^k$, if $E_k(t) \in \bigcup_{i \in I} ({}^{k}E_{31}^i \bigcup {}^{k}E_{12}^i)$;
3) $\dot{E}_k(t) \in \dot{E}_{\mathrm{VA}^-}^k$, if $E_k(t) \in \bigcup_{i \in I} {}^{k}\hat{E}_{21}^i$;
4) $\dot{E}_k(t) \in \dot{E}_{\mathrm{VA}^+}^k$, if $E_k(t) \in \bigcup_{i \in I} {}^{k}\hat{E}_{22}^i$;

5) $\dot{E}_k(t) \in \dot{E}^k_{\mathrm{HD}^-}$, if $E_k(t) \in \bigcup_{i\in I} {}^k\tilde{E}^i_{21}$;
6) $\dot{E}_k(t) \in \dot{E}^k_{\mathrm{HD}^+}$, if $E_k(t) \in \bigcup_{i\in I} {}^k\tilde{E}^i_{22}$.

These following cases are possible based on (18)−(20) and the above conclusions 1)−6).

1) $(k.3.j_1.3)$ when $E_k(t) \in {}^kE^3_{3j_1}$, the trajectory of $E_k(t)$ will reach the sliding manifold ${}^k\Sigma^3_{j_1}$, or move from ${}^kE^3_{3j_1}$ into ${}^kE^2_{3j_1}$, then the case $(k.2.j_1.3)$ holds.

2) $(k.2.j_1.3)$ when $E_k(t) \in {}^kE^2_{3j_1}$, the trajectory of $E_k(t)$ will reach the sliding manifold ${}^k\Sigma^2_{j_1}$, or move from ${}^kE^2_{3j_1}$ into ${}^kE^1_{3j_1}$, then the case $(k.1.j_1.3)$ holds.

3) $(k.1.j_1.3)$ when $E_k(t) \in {}^kE^1_{3j_1}$, the trajectory of $E_k(t)$ will reach the sliding manifold ${}^k\Sigma^1_{j_1}$, or move from ${}^kE^1_{3j_1}$ into ${}^kE^1_{1j_2}$, then the case $(k.1.j_2.1)$ holds.

4) $(k.1.j_2.1)$ when $E_k(t) \in {}^kE^1_{1j_2}$, the trajectory of $E_k(t)$ will move from ${}^kE^1_{1j_2}$ into ${}^kE^1_{2j_2}$, then the case $(k.1.j_2.2)$ holds, or move from ${}^kE^1_{1j_2}$ into ${}^kE^2_{1j_2}$, then the case $(k.2.j_2.1)$ holds.

5) $(k.2.j_2.1)$ when $E_k(t) \in {}^kE^2_{1j_2}$, the trajectory of $E_k(t)$ will move from ${}^kE^2_{1j_2}$ into ${}^kE^2_{2j_2}$, then the case $(k.2.j_2.2)$ holds, or move from ${}^kE^2_{1j_2}$ into ${}^kE^3_{1j_2}$, then the case $(k.3.j_2.1)$ holds.

6) $(k.3.j_2.1)$ when $E_k(t) \in {}^kE^3_{1j_2}$, the trajectory of $E_k(t)$ will move from ${}^kE^3_{1j_2}$ into ${}^kE^3_{2j_2}$, then the case $(k.3.j_2.2)$ holds.

7) $(k.3.j_2.2)$ when $E_k(t) \in {}^kE^3_{2j_2}$, the trajectory of $E_k(t)$ will reach the sliding manifold ${}^k\Sigma^3_{j_2}$, or move from ${}^kE^3_{2j_2}$ into ${}^kE^2_{2j_2}$, then the case $(k.2.j_2.2)$ holds.

8) $(k.2.j_2.2)$ when $E_k(t) \in {}^kE^2_{2j_2}$, the trajectory of $E_k(t)$ will reach the sliding manifold ${}^k\Sigma^2_{j_2}$, or move from ${}^kE^2_{2j_2}$ into ${}^kE^1_{2j_2}$, then the case $(k.1.j_2.2)$ holds.

9) $(k.1.j_2.2)$ when $E_k(t) \in {}^kE^1_{2j_2}$, the trajectory of $E_k(t)$ will reach the sliding manifold ${}^k\Sigma^1_{j_2}$.

There are $j_1 = 1, 2$, $j_2 = 1, 2$, $j_1 \neq j_2$, and $k = 1, 2, \ldots, m$ in these above cases.

Therefore, by virtue of these above cases and the conclusions 1)−6), as well as (16)−(20), it can be concluded that the HNT-SS manifold $s_H = 0$ is reached in finite time.

The reaching time $t_R^{(k)}$ is assumed as the time that is taken to travel from $s_H^{(k)}(0) \neq 0$ to $s_H^{(k)}(t_R^{(k)}) = 0$, and the attaining time $t_S^{(k)}$ is assumed as the time that is taken to travel from $e_k^{(1)}(t_R^{(k)}) \neq 0$ to $e_k^{(1)}(t_R^{(k)} + t_S^{(k)}) = 0$. Once the HNT-SS manifold $s_H^{(k)} = 0$ is reached, there is $\dot{e}_k^{(1)} = -\beta_k \alpha_{i^*}^{(k)} |e_k^{(1)}|^{\gamma_{i^*}^{(k)}} \mathrm{sgn}(e_k^{(1)})$ or $\dot{e}_k^{(1)} = -\beta_k e_k^{(1)}$. By integrating (5), there are following cases below:

1) If $|e_k^{(1)}(t_R^{(k)})| \in [1, +\infty)$,

$$t_S^{(k)} = \frac{1}{\beta_k} \ln |e_k^{(1)}(t_R^{(k)})| + \frac{1}{\beta_k(1-\gamma_2^{(k)})}(1 - \delta_k^{1-\gamma_2^{(k)}}) + \frac{1}{\beta_k(1-\gamma_1^{(k)})}\delta_k^{1-\gamma_2^{(k)}}. \tag{29}$$

2) If $|e_k^{(1)}(t_R^{(k)})| \in [\delta_k, 1)$,

$$t_S^{(k)} = \frac{1}{\beta_k(1-\gamma_2^{(k)})}(|e_k^{(1)}(t_R^{(k)})|^{1-\gamma_2^{(k)}} - \delta_k^{1-\gamma_2^{(k)}}) + \frac{1}{\beta_k(1-\gamma_1^{(k)})}\delta_k^{1-\gamma_2^{(k)}}. \tag{30}$$

3) If $|e_k^{(1)}(t_R^{(k)})| \in [0, \delta_k)$,

$$t_S^{(k)} = \frac{1}{\beta_k \alpha_1^{(k)}(1-\gamma_1^{(k)})} |e_k^{(1)}(t_R^{(k)})|^{1-\gamma_1^{(k)}}. \tag{31}$$

Therefore, it is concluded that the HNT-SS manifold can be reached in finite time and furthermore the state will converge to the equilibrium in finite time.

## IV. Performance Analysis

The performance of the proposed approach is presented in this section. The property of global high-speed convergence is studied through comparing with the NFTSM.

The NFTSM is described as follows:

$$\begin{cases} \sigma_1 = e_1 \\ \sigma_2 = \sigma_1 + \frac{\hat{\beta}}{2-\hat{\gamma}} |\dot{\sigma}_1 + \hat{c}\sigma_1|^{2-\hat{\gamma}} \mathrm{sgn}(\dot{\sigma}_1 + \hat{c}\sigma_1) \end{cases} \tag{32}$$

where $\hat{\beta} > 0$, $\hat{c} > 0$, $\hat{\gamma} = \hat{z}_1/\hat{z}_2$ and $0 < \hat{z}_1 < \hat{z}_2$. The equivalent form of (32) is given by

$$\dot{e}_1 = -\alpha_{_{NF}} e_1 - \beta_{_{NF}} |e_1|^{\gamma_{NF}} \mathrm{sgn}(e_1) \tag{33}$$

where $\alpha_{_{NF}} = \hat{c}$, $\beta_{_{NF}} = (\frac{2-\hat{\gamma}}{\hat{\beta}})^{\frac{1}{2-\hat{\gamma}}}$ and $\gamma_{_{NF}} = \frac{1}{2-\hat{\gamma}} \in (0.5, 1)$.

When sliding manifolds are reached, for the HNT-SSM, there is $\dot{e}_k^{(1)} = -\beta_k \alpha_{i^*}^{(k)} |e_k^{(1)}|^{\gamma_{i^*}^{(k)}} \mathrm{sgn}(e_k^{(1)})$ or $\dot{e}_k^{(1)} = -\beta_k e_k^{(1)}$; for the NFTSM, there is (33). If $\beta_k = \alpha_{_{NF}} + \beta_{_{NF}}$, then, for $e_k^{(1)} = e_1$ and $|e_k^{(1)}| = |e_1| \in (1, +\infty)$, there is

$$\begin{aligned} |-\beta_k e_k^{(1)}| &= |-\alpha_{_{NF}} e_k^{(1)} - \beta_{_{NF}} e_k^{(1)}| \\ &> |-\alpha_{_{NF}} e_1 - \beta_{_{NF}} |e_1|^{\gamma_{NF}} \mathrm{sgn}(e_1)| \end{aligned} \tag{34}$$

for $e_k^{(1)} = e_1$ and $|e_k^{(1)}| = |e_1| \in [\delta_k, 1)$, there is

$$\begin{aligned} &\left| -\beta_k \alpha_2^{(k)} \left| e_k^{(1)} \right|^{\gamma_2^{(k)}} \mathrm{sgn}\left(e_k^{(1)}\right) \right| \\ &\quad = \left| -\alpha_{_{NF}} \left| e_k^{(1)} \right|^{\gamma_2^{(k)}} \mathrm{sgn}\left(e_k^{(1)}\right) \right. \\ &\qquad \left. -\beta_{_{NF}} \left| e_k^{(1)} \right|^{\gamma_2^{(k)}} \mathrm{sgn}\left(e_k^{(1)}\right) \right| \\ &\quad > |-\alpha_{_{NF}} e_1 - \beta_{_{NF}} |e_1|^{\gamma_{NF}} \mathrm{sgn}(e_1)| \end{aligned} \tag{35}$$

for $e_k^{(1)} = e_1$ and $|e_k^{(1)}| = |e_1| \in (0, \delta_k)$ with $\gamma_1^{(k)} = \gamma_{_{NF}}$, there is

$$\begin{aligned} &\left| -\beta_k \alpha_1^{(k)} |e_k^{(1)}|^{\gamma_1^{(k)}} \mathrm{sgn}(e_k^{(1)}) \right| \\ &\quad = \left| -\alpha_{_{NF}} \delta_k^{\gamma_2^{(k)} - \gamma_1^{(k)}} |e_k^{(1)}|^{\gamma_1^{(k)}} \mathrm{sgn}(e_k^{(1)}) \right. \\ &\qquad \left. -\beta_{_{NF}} \delta_k^{\gamma_2^{(k)} - \gamma_1^{(k)}} |e_k^{(1)}|^{\gamma_1^{(k)}} \mathrm{sgn}(e_k^{(1)}) \right| \\ &\quad > \left| -\alpha_{_{NF}} e_1 - \beta_{_{NF}} |e_1|^{\gamma_{NF}} \mathrm{sgn}(e_1) \right|. \end{aligned} \tag{36}$$

It is presented that the proposed approach possesses the property of global high-speed convergence.

It is also noted that the proposed approach avoids the singularity since $e_k^{(1)} \neq 0$ for $E_k(t) \in E_2^k$, and $\gamma_1^{(k)} > 0.5$ for $E_k(t) \in E_1^k$.

## V. Numerical Example

To illustrate the theoretical analysis and the effectiveness of the proposed approach, the HNT-SSMC is compared with the NFTSMC which is designed according to [26].

Here, the elements in (1) are as follows [5]:

$$M_{11}(q) = (m_1 + m_2)r_1^2 + m_2 r_2^2 + 2m_2 r_1 r_2 \cos(q_2) + J_1$$
$$M_{12}(q) = M_{21}(q) = m_2 r_2^2 + m_2 r_1 r_2 \cos(q_2)$$
$$M_{22}(q) = m_2 r_2^2 + J_2$$
$$C(q, \dot{q}) = \begin{bmatrix} -m_2 r_1 r_2 \sin(q_2)\dot{q}_1^2 - 2m_2 r_1 r_2 \sin(q_2)\dot{q}_1\dot{q}_2 \\ m_2 r_1 r_2 \sin(q_2)\dot{q}_2^2 \end{bmatrix}$$
$$G(q) = \begin{bmatrix} (m_1 + m_2)r_1 \cos(q_2)g + m_2 r_2 \cos(q_1 + q_2)g \\ m_2 r_2 \cos(q_1 + q_2)g \end{bmatrix}$$
$$\tau_d = \begin{bmatrix} 2\sin(t) + 0.5\sin(200\pi t) \\ \cos(2t) + 0.5\sin(200\pi t) \end{bmatrix}$$

The parameter values are $r_1 = 1$, $r_2 = 0.8$, $J_1 = 5\,\text{kg·m}$, $J_2 = 5\,\text{kg·m}$, $m_1 = 0.5\,\text{kg}$, $m_2 = 1.5\,\text{kg}$. The normal values of $m_1$ and $m_2$ are assumed to be $m_{10} = 0.4\,\text{kg}$, $m_{20} = 1.2\,\text{kg}$. The desired reference signals are given by $q_{1r} = 1.25 - (7/5)e^{-t} + (7/20)e^{-4t}$, $q_{2r} = 0.25 + e^{-t} - (1/4)e^{-4t}$. The initial values of the system are selected as $q_1(0) = 2.8$, $q_2(0) = 3.0$, $\dot{q}_1(0) = 0.0$, $\dot{q}_2(0) = 0.0$. $b_0 = 9.5$, $b_1 = 2.2$, and $b_2 = 2.8$ is assumed.

The parameters of the HNT-SSMC (3) and the NFTSMC are $\beta_k = 1$, $\gamma_1^{(k)} = 0.69$, $\gamma_2^{(k)} = 0.1$, $\delta_k = 0.15$, $\hat{\beta}_k = 3.85$, $\hat{c}_k = 0.50$, $\hat{\gamma}_k = 0.57$, $k = 1, 2$. Thus there is $\beta_k = \alpha_{NFk} + \beta_{NFk}$ $(k = 1, 2)$. The boundary layer method is adopted to eliminate chattering.

It can be found that the proposed approach can offer higher convergence speed (see Fig. 3−5), realize different control targets in the different regions of state space (see Figs. 6 and 7), and both of the requirements are fulfilled by switching among appropriate sliding mode controllers (see Figs. 8 and 9). It can also be noticed that neither singularity nor chattering occurs in the two control inputs of HNT-SSMC during the whole control process (see Fig. 8).

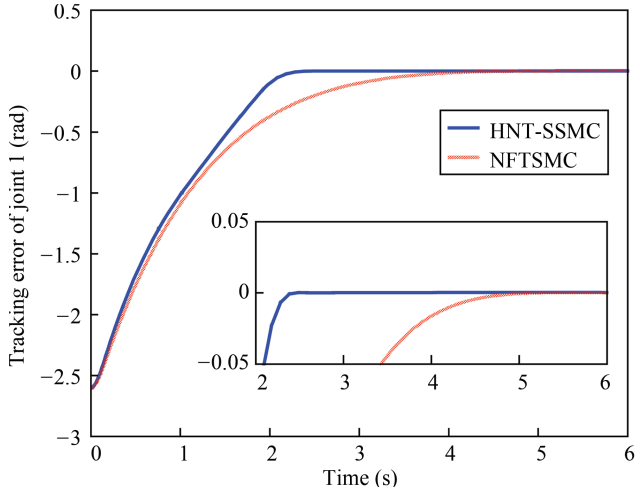


Fig. 3. Tracking error of joint 1.

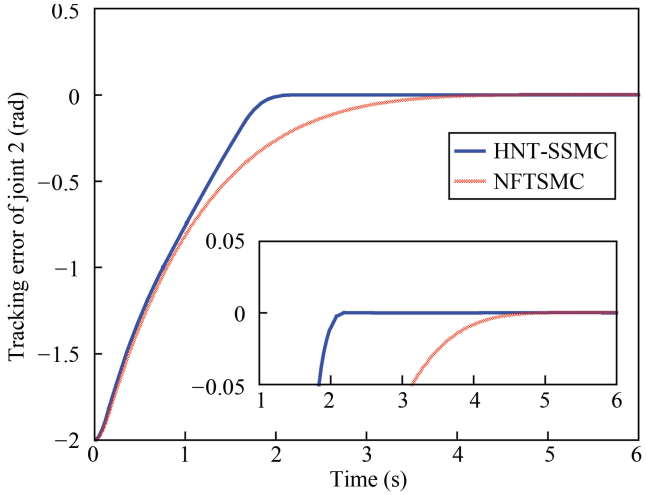


Fig. 4. Tracking error of joint 2.

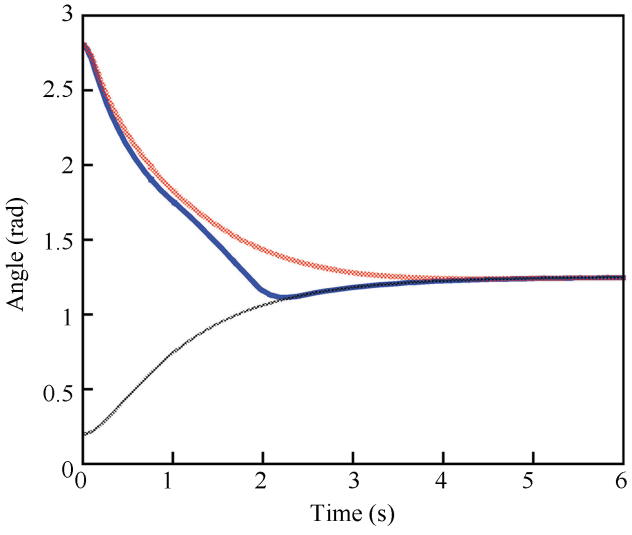


(a)

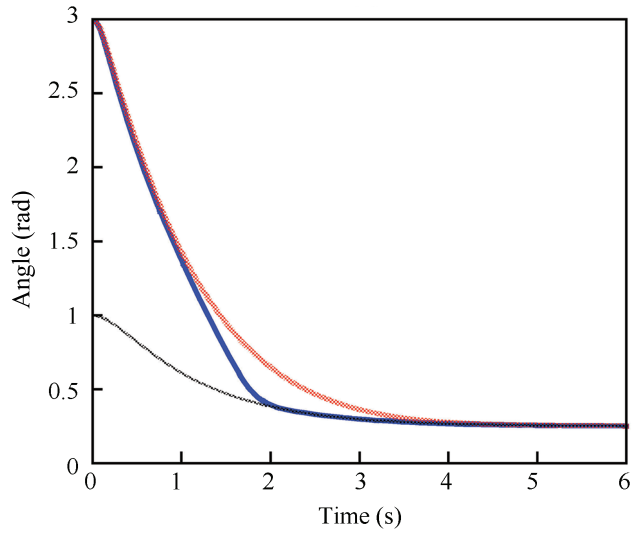


(b)

Fig. 5. Output tracking of joints. (a) joint 1: $q_1$ with HNT-SSMC (blue), $q_1$ with NFTSMC (red), $q_{1r}$ (black). (b) joint 2: $q_2$ with HNT-SSMC (blue), $q_2$ with NFTSMC (red), $q_{2r}$ (black).

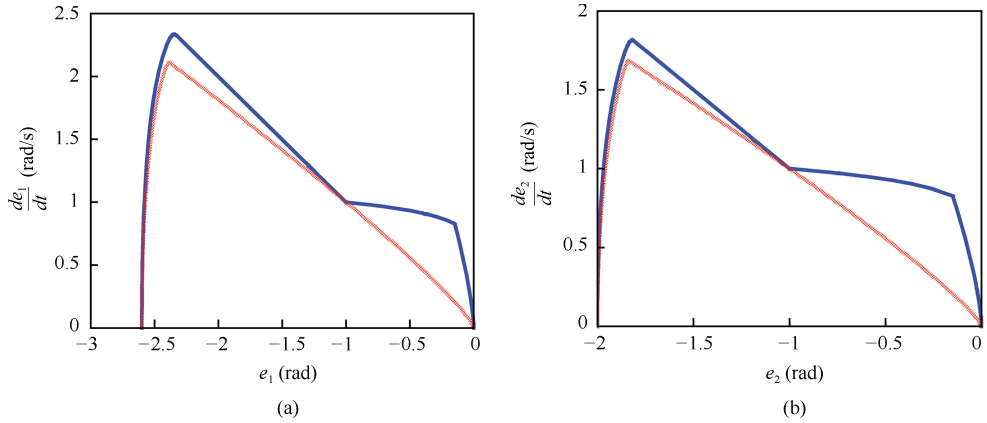


Fig. 6. Phase plots of tracking errors of joints. (a) joint 1: with HNT-SSMC (blue), with NFTSMC (red). (b) joint 2: with HNT-SSMC (blue), with NFTSMC (red).

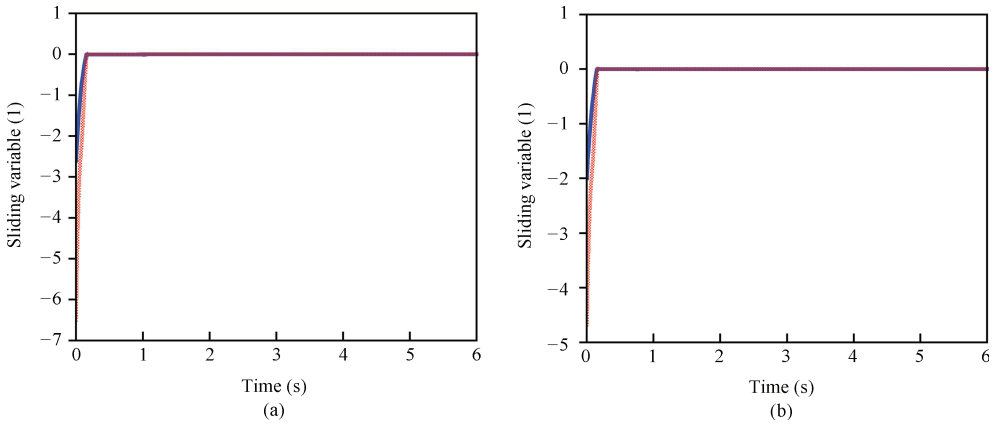


Fig. 7. Sliding variables of joints. (a) joint 1: with HNT-SSMC (blue), with NFTSMC (red). (b) joint 2: with HNT-SSMC (blue), with NFTSMC (red).

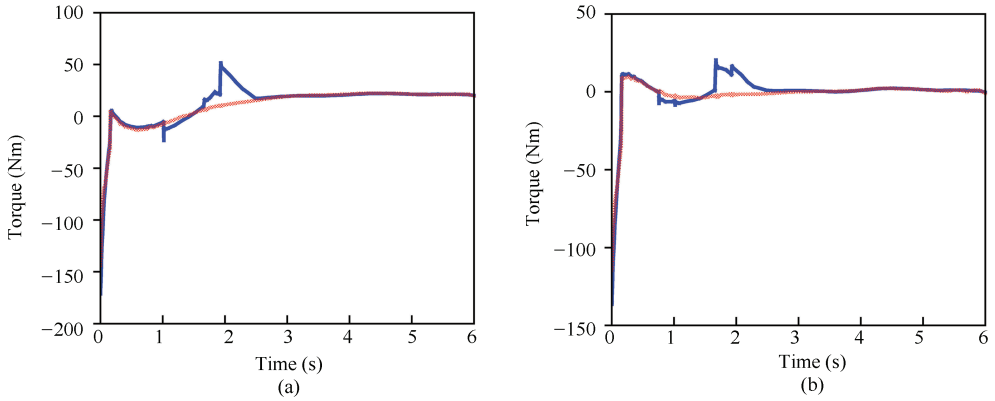


Fig. 8. Control inputs of joints. (a) joint 1: with HNT-SSMC (blue), with NFTSMC (red). (b) joint 2: with HNT-SSMC (blue), with NFTSMC (red).

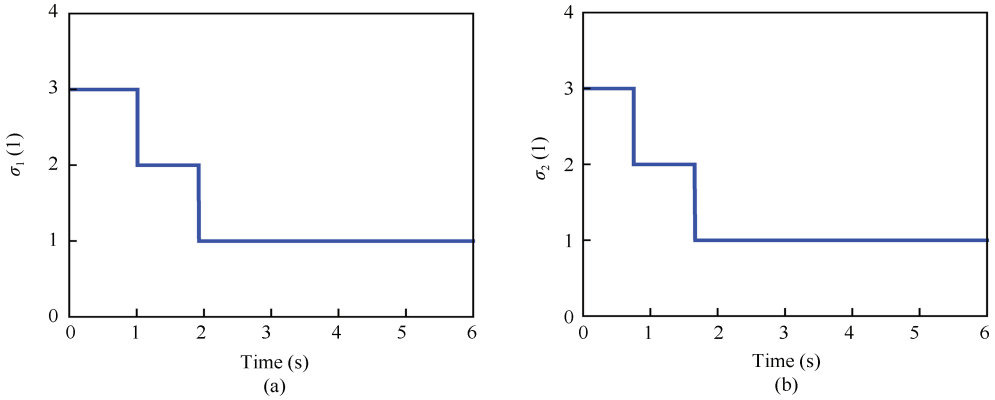


Fig. 9 Switching signals with HNT-SSMC. (a) $\sigma_1$. (b) $\sigma_2$.

## VI. Conclusion

In this paper, the proposed approach for robot manipulators, which schedules sliding mode controllers according to different control demands in the different regions of the state space, allows control performance enhancement. And the HNT-SSM simultaneously has the property of global high-speed convergence, and provides the global non-singularity. Further, the effectiveness of the proposed approach and the theoretical analysis is validated by simulation.

## References


[1] L. Cheng, Z. G. Hou, and M. Tan, "Adaptive neural network tracking control for manipulators with uncertain kinematics, dynamics and actuator model," *Automatica*, vol. 45, no. 10, pp. 2312−2318, Oct. 2009.

[2] L. Cheng, Y. Z. Lin, Z. G. Hou, M. Tan, J. Huang, and W. J. Zhang, "Adaptive tracking control of hybrid machines: A closed-chain five-bar mechanism case," *IEEE/ASME Trans. Mechatron.*, vol. 16, no. 6, pp. 1155−1163, Dec. 2011.

[3] Y. Q. Gao, F. Y. Wang, and Z. Q. Zhao, *Flexible Manipulators: Modeling, Analysis and Optimum Design*. New York: Academic Press, 2012, pp. 185−249.

[4] L. Cheng, Z. G. Hou, M. Tan, and W. J. Zhang, "Tracking control of a closed-chain five-bar robot with two degrees of freedom by integration of an approximation-based approach and mechanical design," *IEEE Trans. Syst. Man Cybern. B Cybern.*, vol. 42, no. 5, pp. 1470−1479, Oct. 2012.

[5] Y. Feng, X. H. Yu, and Z. H. Man, "Non-singular terminal sliding mode control of rigid manipulators," *Automatica*, vol. 38, no. 12, pp. 2159−2167, Dec. 2002.

[6] X. Wang and J. Zhao, "Switched adaptive tracking control of robot manipulators with friction and changing loads," *Int. J. Syst. Sci.*, vol. 46, no. 6, pp. 955−965, May 2015.

[7] H. Lin and P. J. Antsaklis, "Stability and stabilizability of switched linear systems: A survey of recent results," *IEEE Trans. Automat. Control*, vol. 54, no. 2, pp. 308−322, Feb. 2009.

[8] Q. S. Xu, "Design and smooth position/force switching control of a miniature gripper for automated microhandling," *IEEE Trans. Industr Inform.*, vol. 10, no. 2, pp. 1023−1032, May 2014.

[9] F. Blanchini, P. Colaneri, D. Casagrande, P. Gardonio, and S. Miani, "Switching gains for semiactive damping via nonconvex Lyapunov functions," *IEEE Trans. Control Syst. Technol.*, vol. 22, no. 2, pp. 721−728, Mar. 2014.

[10] G. S. Deaecto, M. Souza, and J. C. Geromel, "Discrete-time switched linear systems state feedback design with application to networked control," *IEEE Trans. Automat. Control*, vol. 60, no. 3, pp. 877−881, Mar. 2015.

[11] X. D. Zhao, P. Shi, and L. X. Zhang, "Asynchronously switched control of a class of slowly switched linear systems," *Syst. Control Lett.*, vol. 61, no. 12, pp. 1151−1156, Dec. 2012.

[12] Y. Feng, F. L. Han, and X. H. Yu, "Chattering free full-order sliding-mode control," *Automatica*, vol. 50, no. 4, pp. 1310−1314, Apr. 2014.

[13] J. J. Slotine and W. P. Li, *Applied Nonlinear Control*. Englewood Cliffs, NJ: Prentice-Hall, 1991, pp. 276−310.

[14] G. Bartolini and E. Punta, "Multi-input sliding mode control of nonlinear uncertain non-affine systems with mono-directional actuation," *IEEE Trans. Automat. Control*, vol. 60, no. 2, pp. 393−403, Feb. 2015.

[15] X. G. Yan, S. K. Spurgeon, and C. Edwards, "Memoryless static output feedback sliding mode control for nonlinear systems with delayed disturbances," *IEEE Trans. Automat. Control*, vol. 59, no. 7, pp. 1906−1912, Jul. 2014.

[16] M. Rubagotti, A. Estrada, F. Castanos, A. Ferrara, and L. Fridman, "Integral sliding mode control for nonlinear systems with matched and unmatched perturbations," *IEEE Trans. Automat. Control*, vol. 56, no. 11, pp. 2699−2704, Nov. 2011.

[17] O. Barambones and P. Alkorta, "Position control of the induction motor using an adaptive sliding-mode controller and observers," *IEEE Trans. Industr. Electron.*, vol. 61, no. 12, pp. 6556−6565, Dec. 2014.

[18] R. M. Zhang, L. Dong, and C. Y. Sun, "Adaptive nonsingular terminal sliding mode control design for near space hypersonic vehicles," *IEEE/CAA J. Automat. Sin.*, vol. 1, no. 2, pp. 155−161, Apr. 2014.

[19] J. M. Zhang, C. Y. Sun, R. M. Zhang, and C. S. Qian, "Adaptive sliding mode control for re-entry attitude of near space hypersonic vehicle based on backstepping design," *IEEE/CAA J. Automat. Sin.*, vol. 2, no. 1, pp. 94 −101, Jan. 2015.

[20] C. X. Mu, Q. Zong, B. L. Tian, and W. Xu, "Continuous sliding mode controller with disturbance observer for hypersonic vehicles," *IEEE/CAA J. Automat. Sin.*, vol. 2, no. 1, pp. 45−55, Jan. 2015.

[21] H. Ríos, S. Kamal, L. M. Fridman, and A. Zolghadri, "Fault tolerant control allocation via continuous integral sliding-modes: A HOSM-Observer approach," *Automatica*, vol. 51, pp. 318−325, Jan. 2015.

[22] T. Bernardes, V. F. Montagner, H. A. Grundling, and H. Pinheiro, "Discrete-time sliding mode observer for sensorless vector control of permanent magnet synchronous machine," *IEEE Trans. Industr. Electron.*, vol. 61, no. 4, pp. 1679−1691, Apr. 2014.

[23] I. Nagesh and C. Edwards, "A multivariable super-twisting sliding mode approach," *Automatica*, vol. 50, no. 3, pp. 984−988, Mar. 2014.

[24] Z. H. Man, A. P. Paplinski, and H. R. Wu, "A robust MIMO terminal sliding mode control scheme for rigid robotic manipulators," *IEEE Trans. Automat. Control*, vol. 39, no. 12, pp. 2464−2469, Dec. 1994.

[25] X. H. Yu and Z. H. Man, "Fast terminal sliding-mode control design for nonlinear dynamical systems," *IEEE Trans. Circuits Syst. I Fundam. Theory Appl.*, vol. 49, no. 2, pp. 261−264, Feb. 2002.

[26] H. Li, L. H. Dou, and Z. Su, "Adaptive nonsingular fast terminal sliding mode control for electromechanical actuator," *Int. J. Syst. Sci.*, vol. 44, no. 3, pp. 401−415, Aug. 2013.


**Fengning Zhang** graduated from Harbin Engineering University, China, in 2005. He received the master degree from Harbin Institute of Technology, China, in 2008. He is currently a Lecturer in the Department of Physics, Jining Normal University. His research interests include switched control, sliding mode control, and robotics.